Contribution of the PI3K/MMPs/Ln-5γ2 and EphA2/FAK/Paxillin signaling pathways to tumor growth and vasculogenic mimicry of gallbladder carcinomas

XIN-SUI LU[1*], WEI SUN[2*], CHUN-YAN GE[1*], WEN-ZHONG ZHANG[1] and YUE-ZU FAN[1]

[1]Department of Surgery, Tongji Hospital, Tongji University School of Medicine; [2]Department of Surgery, Shanghai Tenth People's Hospital, Tongji University, Shanghai, P.R. China

Received February 1, 2013; Accepted March 26, 2013

DOI: 10.3892/ijo.2013.1897

Abstract. Vasculogenic mimicry (VM) is a new tumor blood supply in some highly aggressive malignant tumors. We previously reported VM in human gallbladder carcinomas, 3-D matrices *in vitro* and nude mouse xenografts *in vivo* of highly aggressive GBC-SD cells and its clinical significance. In this study, we further studied the underlying mechanisms of VM in gallbladder carcinomas via the 3-D matrix *in vitro*, the nude mouse xenografts *in vivo* of GBC-SD or SGC-996 cells, immunohistochemistry (H&E staining and CD31-PAS double staining), electron microscopy, expression of MMP-2, MT1-MMP, PI3K, Ln-5γ2, EphA2, FAK and Paxillin-P proteins/mRNAs determined by SABC, ELISA, immunofluorescence, western blotting and qRT-PCR, respectively. It was shown that all of untreated highly aggressive GBC-SD cells and xenografts formed vasculogenic-like structures within 2 weeks of seeding and injecting, and facilitated the growth of tumor cells or xenografts; whereas poorly aggressive SGC-996 cells or GBC-SD cells treated by TIMP-2 were unable to form the vasculogenic-like structures with the same conditions; and tumor xenograft growth was inhibited. Expression of MMP-2, MT1-MMP proteins/mRNAs from sections and supernates of 3-D matrix *in vitro*, expression of PI3K, MMP-2, MT1-MMP, Ln-5γ2, EphA2, FAK and Paxillin-P proteins/mRNAs from sections of xenografts *in vivo* in untreated GBC-SD group was upregulated significantly (all $P<0.001$); however, expression of these VM signal-related proteins/mRNAs in the SGC-996 group and GBC-SD treated by the TIMP-2 group was significantly downregulated (all $P<0.001$). Thus, we identified for the first time that highly aggressive GBC-SD cells formed VM *in vitro* and *in vivo* through the upregulation of PI3K/MMPs/Ln-5γ2 and/or EphA2/FAK/Paxillin signaling. PI3K/MMPs/Ln-5γ2 and EphA2/FAK/Paxillin as key signaling pathways in a coordinated manner contributed to tumor growth and VM of gallbladder carcinomas and provided novel targets that could be potentially exploited for therapeutic intervention of human gallbladder carcinomas.

Correspondence to: Professor Yue-Zu Fan, Department of Surgery, Tongji Hospital, Tongji University School of Medicine, 389 Xincun Road, Shanghai 200065, P.R. China
E-mail: fanyuezu_shtj@yahoo.com.cn

*Contributed equally

Abbreviations: VM, vasculogenic mimicry; EphA2, ephrin type a receptor 2; FAK, focal adhesion kinase; PI3K, phosphoinositide 3-kinase; MMP, matrix metalloproteinase; MT1-MMP, membrane type 1-MMP; TIMP-2, tissue inhibitor of matrix metalloproteinase-2; Ln-5, laminin 5; VE-cad, vascular endothelial-cadherin; ECM, extracellular matrix; 3-D culture, three-dimensional culture; PAS, periodic acid-Schiff; SABC, streptavidin-biotin complex method; DAB, 3,3-diaminob enzidine; ELISA, enzyme-linked immunosorbent assay; TMB, tetramethylbenzidine; qRT-PCR, quantitative reverse transcription-polymerase chain reaction; SEM, scanning electron microscopy; TEM, transmission electron microscopy

Key words: gallbladder neoplasm, vasculogenic mimicry, 3-dimensional matrix, xenograft model, signaling pathway

Introduction

Gallbladder carcinoma is the most common malignancy of the biliary tract, the fifth or sixth common malignant neoplasm of the digestive tract and the leading cause of cancer-related deaths in West countries and China (1-5). The low 5-year survival rate and poor prognosis of patients with gallbladder carcinoma is related to diagnostic delay, low surgical excision rate, high local recurrence and distant metastasis and biological behavior of the tumor. Additionally, chemotherapy and radiotherapy for the disease are disappointing (1,6-12). Therefore, it is an urgent task to reveal the precise special biological behavior of gallbladder carcinoma development and provide a novel perspective for anticancer therapeutics.

The growth and metastasis of the tumor depend on an effective microcirculation. The formation of a microcirculation can occur via the traditionally recognized mechanisms of vasculogenesis and angiogenesis and the recently found VM. VM, a newly-defined pattern of tumor blood supply, provides a special passage without endothelial cells and is conspicuously different from angiogenesis and vasculogenesis (13) and

is associated with a poor prognosis for the patients with some aggressive malignant tumors such as melanoma (13,14), breast cancer (15), ovarian carcinoma (16), hepatocellular carcinoma (17,18), gastric adenocarcinomas (19), and colorectal cancer (20). However, the detailed mechanism of the tumor cells that form VM remains to be further elucidated. Currently, some signaling pathways involving factors which promote cell migration, invasion and matrix remodeling are thought to relative with the formation of tumor VM. These include PI3K, MMPs, Ln-5γ2 chain (21-24), EphA2, FAK (25-29), tissue factor (TF) and its pathway inhibitor (TFPI) (30) and vascular endothelial growth factor α (VEGFα) (31), and others (32,33). Therefore, understanding the key molecular mechanisms that regulate VM would serve as an important target for new cancer therapies.

We previously reported that VM existed in human gallbladder carcinomas and gallbladder carcinomas by both 3-D matrices of highly aggressive GBC-SD cells *in vitro* and GBC-SD nude mouse xenografts *in vivo* and correlated with the patient's poor prognosis and that poorly aggressive SGC-996 cells did not form the vasculogenic-like networks when cultured under the same conditions, but formed pattern, vasculogenic-like networks when being cultured on a matrix preconditioned by the GBC-SD cells (34-36). However, the exact mechanism underlying VM in gallbladder carcinomas still needs to be unraveled. In this study, we firstly present evidence that the formation of VM in human gallbladder carcinomas through the activation of the EphA2/FAK/Paxillin signaling pathway and the PI3K/MMPs/Ln-5γ2 signaling pathway in the 3-D matrixes of GBC-SD cells *in vitro* and GBC-SD nude mouse xenografts *in vivo* and provide a potential target therapy for VM of gallbladder carcinomas.

Materials and methods

Cell culture. Human gallbladder carcinoma (GBC-SD and SGC-996) cell lines have been described previously (36) and were maintained in Dulbecco's modified Eagle's media (DMEM, Gibco Co., USA) supplemented with 10% fetal bovine serum (FBS, Hangzhou Sijiqing Bioproducts, China) and 10^5 U/ml penicillin and streptomycin (Shanghai Pharmaceutical Works, China) in an incubator (Forma series II HEPA Class 100, Thermo Co., USA) at 37˚C with 5% carbon dioxide (CO_2).

Network formation assay in vitro. Matrigel and rat-tail collagen type I three dimensional matrices were prepared as described previously (36). Cells were allowed to adhere to the matrix and untreated and treated with 100 nM TIMP-2 recombinant protein (Sigma Co., Germany) for 4 days. Phase contrast microscopy (Olympus IX70, Japan) was used for analyzing the ability of the cells to engage in VM. The images were taken digitally using a Zeiss Televal inverted microscope (Carl Zeiss, Inc., Thornwood, NY) and camera (Nikon, Japan) at the time indicated.

Tumor xenograft assay in vivo. Balb/c nu/nu mice (equal numbers of male and female mice, 4-week old, ~20 g) were provided by Shanghai Laboratory Animal Center, Chinese Academy of Sciences and housed in specific pathogen-free (SPF) conditions. All the procedures were performed on nude mice according to the official recommendations of the Chinese Community Guidelines. Tumor xenograft assay of GBC-SD and SGC-996 cells *in vivo* was performed as described previously (36). The mice, by 2 weeks when a tumor xenograft was apparent in the axilback of all mice, were randomly divided into a GBC-SD group (n=7), a SGC-996 group (n=7) receiving intraperitoneal injections of 0.1 ml normal saline alone twice each week and a GBC-SD+TIMP-2 group (n=6, each mouse with GBC-SD xenograft receiving intratumoral injection of 100 nM TIMP-2 recombinant protein), twice each week for 6 weeks in all. The maximum diameter (a) and minimum diameter (b) of the xenografts were measured with calipers two times each week. The tumor volume was calculated by the following formula: V (cm^3) = $1/6\pi ab^2$. Also, tumor growth curve of each group was respectively evaluated.

Immunohistochemistry in vitro and in vivo. Immunohistochemistry *in vitro* and *in vivo* included H&E staining, PAS staining, CD31-PAS double staining and the determination of MMP-2 or MT1-MMP protein for sections and supernates from the cell culture tissues and sections of tumor xenografts. i) H&E staining, PAS stainings and CD31-PAS double staining were performed as described previously (36). ii) MMP-2 and MT1-MMP proteins from sections of 3-D culture samples and tumor xenografts were determined by SABC method. The sections (4-μm) from each group were dehydrated in xylene and graded ethanol series, were added in order with primary antibody [MMP-2 (1: 200), MT1-MMP (1:100); rabbit polyclonal antibody, Wuhan Boster Co., China)], biotinylated secondary antibody, SABC reagents and DAB solution (Wuhan Boster Co.), respectively. Then, sections were rinsed in distilled water, dehydrated through alcohol and xylene and mounted coverslip using a permanent mount medium and observed under an optical microscope with x10 and 40 objectives (Olympus CH-2, Japan). For negative control, the slides were treated with PBS in place of primary antibody. Ten sample slides in each group were chosen by analysis. More than 10 visual fields were observed or >500 cells were counted per slide. iii) MMP-2 and MT1-MMP proteins from supernates of 3-D culture samples were determined by ELISA. The supernates from each group and the diluted standard solutions were added into 2 multiple wells, 2 zero adjusting wells and a control TMB well. The former two wells were added with biotinylated antibody (MMP-2, ELISA kits, Wuhan Boster Co.; MT1-MMP, ELISA kits, DR, USA), ABC reagents and TMB solution (Wuhan Boster Co.), respectively; the control TMB well did not include reagents. Optical densities at 450 nm were measured using an ELISA reader (Biorad model, Sigma).

Electron microscopy in vitro and in vivo. For SEM and TEM, 3-D culture samples and fresh tumor xenograft tissues (0.5 mm^3) were fixed in cold 2.5% glutaraldehyde in 0.1 mol/l of sodium cacodylate buffer and postfixed in a solution of 1% osmium tetroxide, dehydrated and embedded in a standard fashion. Specimens were subsequently embedded, sectioned and stained by routine means for a Jeol-1230 TEM, or critically point-dried and sputter-coated with gold for a Hitachi S-520 SEM.

Table I. VM signaling-related markers.

Gene	PCR primers (forward-reverse)	Amplification size (bp)	Cycle no.
MMP-2	5'-AAGAGCGTGAAGTTTGGAAGCA-3' 5'-TCTGAGGGTTGGTGGGATTGG-3'	290	35
MT1-MMP	5'-CAAAGGCAGAACAGCCAGAGG-3' 5'-ACAGGGACCAACAGGAGCAAG-3'	180	35
EphA2	5'-TTAGGGAGAAGGATGGTGAGTT-3' 5'-GTTGCTGTTGACGAGGATGTT-3'	140	35
FAK	5'-CCCAGAAAGAAGGTGAACG-3' 5'-GGTCGAGGGCATGGTGTA-3'	152	35
PI3K	5'-TGTCGCAGCCCAGGTAGATT-3' 5'-CAGGAGGTGGTCGGGTCAAG-3'	269	35
Ln-5γ2	5'-ACACGGGAGATTGCTACTCG-3' 5'-ACCCATTGTGACAGGGACAT-3'	123	35
Paxillin-P	5'-CTTCAAGGAGCAGAACGACAAA-3' 5'-TAGCAGGTGGTAGGGACGAGA-3'5	228	35
GAPDH	5'-CCTCTATGCCAACACAGTGC-3' 5'-GTACTCCTGCTTGCTGATCC-3'	211	35-40

Immunofluorescence detection in vivo. EphA2, FAK, PI3K, Ln-5γ2 and Paxillin-P protein products from the xenografts of each group were determined by indirect immunofluorescence method. The frozen sections (4 μm) of the xenografts from each group were pretreated with 99.5% acetone, methanol with 3% hydrogen peroxide and 20% normal goat serum, were added with 50 μl (1:100) primary antibody [EphA2 and FAK, rabbit anti-human polyclonal antibody, Santa Cruz, USA; PI3K, mouse anti-human polyclonal antibody, Acris Antibodies GmbH, USA; Ln-5γ2, mouse anti-human polyclonal antibody, Santa Cruz; Paxillin (phosphor Y118), rabbit anti-human polyclonal antibody, Abcam Plc, USA], biotinylated secondary antibody (1:100; goat anti-rabbit IgG-FITC/GGHL-15F, or goat anti-mouse IgG-FITC/GGHL-90F, Immunology Consultants Laboratory, USA), respectively. Then, sections were rinsed in TBS solution and distilled water, mounted with coverslip using buffer glycerine and observed under a fluorescence microscope (Nikon, Japan). For negative control, the slides were treated with PBS in place of primary antibody. Ten sample slides in each group were chosen by analysis. More than 10 visual fields were observed per slide. Expression of each protein on slides of the xenografts showed a fluorescent yellow-green stain. Fluorescent stain intensity was classed into -, ±, +, ++, +++, ++++. Of these, - to +, negative expression; ≥++, positive expression.

Western blot analysis in vivo. EphA2, FAK, PI3K, Ln-5γ2 and Paxillin-P proteins from the xenografts of each group were determined by western blot analysis. Cells were lysed with 200 ml of cell lysis buffer (protein extraction kit, KangChen, KC-415, China) containing a cocktail of protease inhibitors and the supernatant of the lysed cells was recovered. BCA protein quantitative determination was carried out with a protein quantitative kit (KangChen, KC-430; China). Then, an aliquot of 20 mg of proteins was subjected to sodium dodecyl sulfate-polyacrylamide gel electrophoresis (SDS-PAGE) under reducing condition and were subsequently transferred to a PVDF membrane. An hour after being blocked with PBS containing 5% non-fat milk, the membrane was incubated overnight, then each primary antibody was added [EphA2, FAK, Ln-5γ2 (all from Santa Cruz); PI3K (P85-a, Acris Antibodies GmbH); Paxillin (phosphor Y118, Abcam Plc): mouse anti-human antibody, 1:3,000; and GAPDH (mouse anti-human antibody, 1:10,000; Kangcheng Bioengineering Co., Shanghai, China) diluted with PBST containing 5% non-fat milk at 4˚C], an appropriate anti-mouse or anti-rabbit HRP-labeled secondary antibody (1:5,000; Kangcheng Bioengineering Co.). The target proteins were visualized by an enhanced chemiluminescent (ECL) reagent (KC™ Chemiluminescent kit, KangChen, KC-420, China), and imaged on the Bio-Rad chemiluminescence imager. The gray value and gray coefficient ratio of each protein was analyzed and calculated with Image J analysis software.

QRT-PCR analysis in vivo. Expression of MMP-2, MT1-MMP, EphA2, FAK, PI3K, Ln-5γ2 and Paxillin-P mRNAs from the xenografts of each group was respectively determined by qRT-PCR assay. QRT-PCR was performed as described by the manufacturer. Total RNA from the xenograft cells of each group was prepared using the TRizol reagent (Invitrogen, USA). Concentration of RNA was determined by the absorption at 260-280. PCR amplifications were performed with gene-specific primers (Table I) with annealing temperature and number of amplification cycles optimized using cDNA

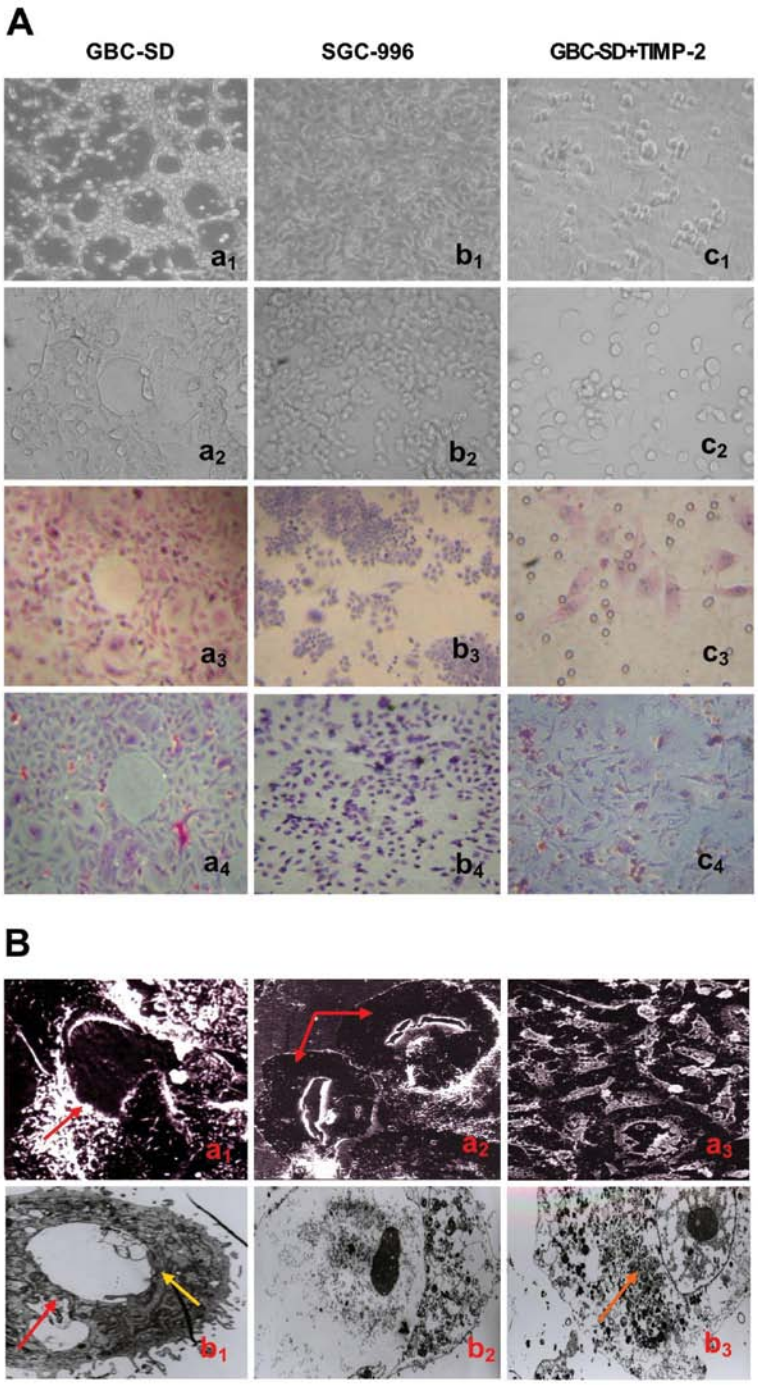

Figure 1. Phase contrast microscopy and electron microscopy on 3-D cultures of GBC-SD and SGC-996 cells *in vitro*. (A) Phase contrast microscopy of GBC-SD cells cultured three dimensionally on Matrigel (a_1, b_l and c_1, original magnification, x200) and rat-tail type I collagen matrix (a_{2-4}, b_{2-4} and c_{2-4}, original magnification, x200) *in vitro*. Highly aggressive GBC-SD cells formed patterned, vasculogenic-like networks when cultured on Matrigel (a_1) and rat-tail type I collagen matrix (a_2 and a_3, H&E staining) for 14 days. Similarly, the 3-D cultures of GBC-SD cells when stained with PAS without hematoxylin counterstain showed the vasculogenic-like structures; PAS-positive, cherry-red materials were found in granules and patches in the cytoplasm of GBC-SD cells appeared around the signal cell or cell clusters (a_4). However, poorly aggressive SGC-996 cells did not form these networks when cultured under the same conditions (b_{1-4}). In the process of network formation, using TIMP-2 for 2 days, GBC-SD cells lost the capacity of the vasculogenic-like network formation, with visible cell aggregation, floating, nuclear fragmentation, apoptosis and necrosis (c_{1-4}). (B) Vasculogenic-like microstructures on 3-D cultures of GBC-SD cells by electron microscopy ($Ba_{1-3,}$ SEM x500; Bb_{1-3}, TEM x1200). SEM clearly visualized channelized or hollowed vasculogenic-like networks formed in GBC-SD cells ($Ba_{1,2}$, red arrowhead), with clear microvillus surrounding cluster of tumor cells. TEM shows some microvilli outside the network, clear cellular organelle structures and cell connection with an increased electron density (Bb_1, yellow arrowhead). After using TIMP-2 for 2 days, GBC-SD cells did not grow along the collagen framework, were raised and deformed, lost the capacity of network formation (Ba_3), with visible decreased microvillus, destroyed cellular organelles, nuclear fragmentation, vacuolar degeneration and typical apoptotic bodies ($Bb_{2,3}$, brown arrowhead).

from the xenograft cells of each group. PCR amplification reactions were performed as follows: 1 cycle of 94˚C for 5 min; 35 cycles of 94˚C for 10-22 sec, 57-60˚C for 15-20 sec, 72˚C for 20 sec, 82-86˚C (fluorescence collection) for 5-10 sec; 1 cycle of 72-99˚C for 5 min. GAPDH primers were used as control for PCR amplification. PCR products (10 μl) were placed

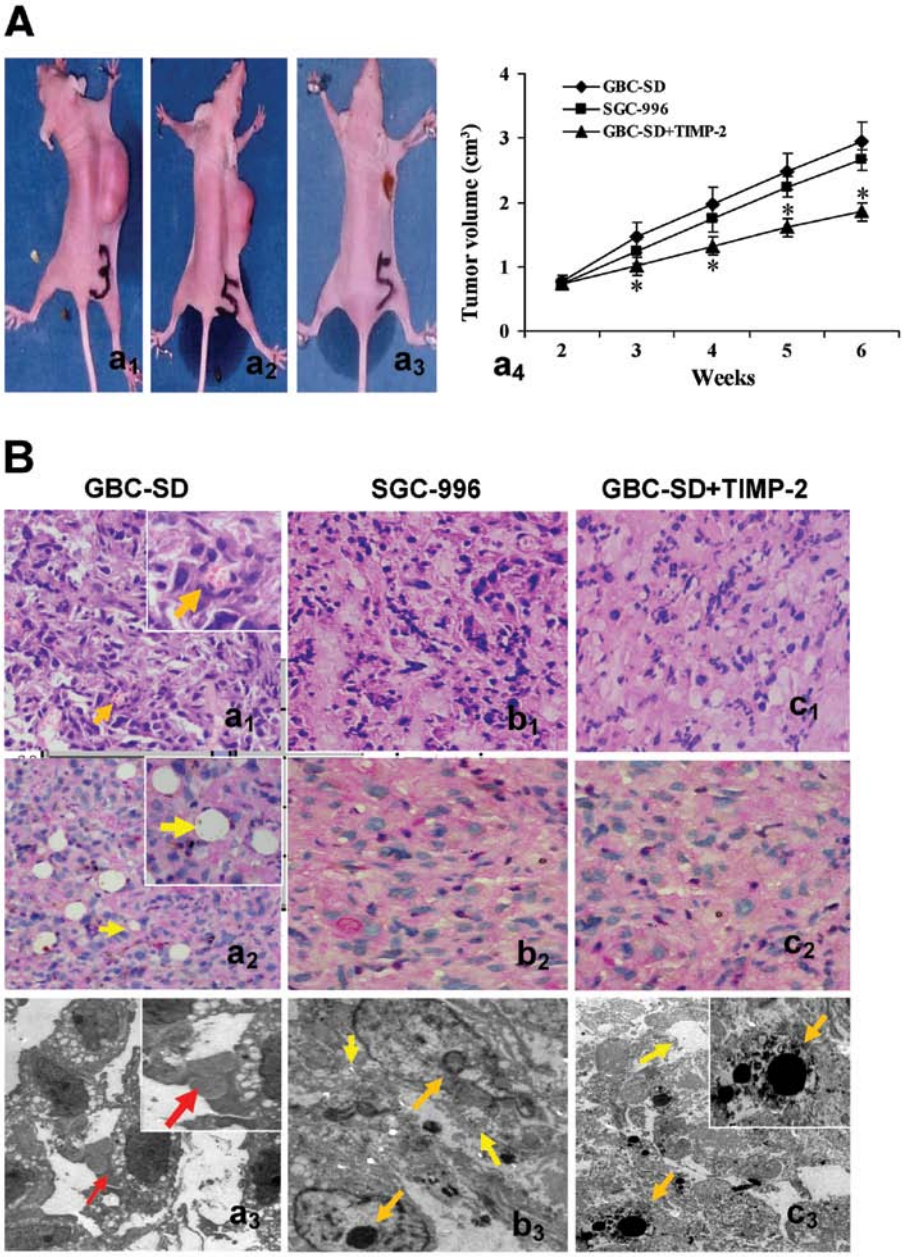

Figure 2. Growth and characteristic appearance of GBC-SD and SGC-996 xenografts *in vivo*. (A) The xenografts of GBC-SD (a_1), SGC-996 (a_2) and GBC-SD+TIMP-2 (a_3, the xenografts exhibited different degree of necrosis, red arrowhead) groups and tumor growth curve in each group (*P<0.001, vs. GBC-SD group or SGC-996 group (a_4). (B) Histomorphologic appearance of the xenografts in GBC-SD (a_{1-3}), SGC-996 (b_{1-3}) and GBC-SD+TIMP-2 (c_{1-3}) groups. Using H&E (a_1, b_1 and c_1) and CD31-PAS double stain (a_2, b_2 and c_2, all original magnification, x200), sections of the xenografts in GBC-SD group showed tumor cell-lined channels containing red blood cells (a_1, orange arrowhead) without any evidence of tumor necrosis; PAS-positive substances line the channel-like structures; tumor cells form vessel-like structure with single red blood cell inside (a_2, yellow arrowhead). TEM (original magnification, x8,000) clearly visualized several red blood cells in the central tumor nests in the xenografts of GBC-SD group (a3, red arrowhead). However, similar phenomenon failed to occur in the xenografts of SGC-996 group (b_{1-3}) or GBC-SD+TIMP-2 (c_{1-3}) group, with destroyed cellular organelles, cell necrosis (b_3 and c_3, yellow arrowhead), nuclear pyknosis, fragmentation and apoptotic bodies (b_3 and c_3, orange arrowhead).

onto 15 g/l agarose gel and observed by ethidium bromide (EB, Huamei Bioengineering Co., China) staining using the ABI PRISM 7300 SDS software.

Statistical analysis. The data are expressed as mean ± SD and performed using SAS, 9.0 version software (SAS Institute Inc., Cary, NC, USA). Statistical analyses to determine significance were tested with the χ^2, F or Student-Newman-Keuls t-tests. P<0.05 was considered statistically significant.

Results

Vasculogenic-like network formation of GBC-SD cells in vitro. As showed in Fig. 1, highly aggressive GBC-SD cells were able to form vasculogenic-like network structures when cultured on Matrigel and rat-tail collagen type I composed of the ECM gel in the absence of endothelial cells and fibroblasts (Fig. 1Aa_{1-4}). The tumor-formed networks initiated formation within 48 h after seeding the cells onto the matrix with

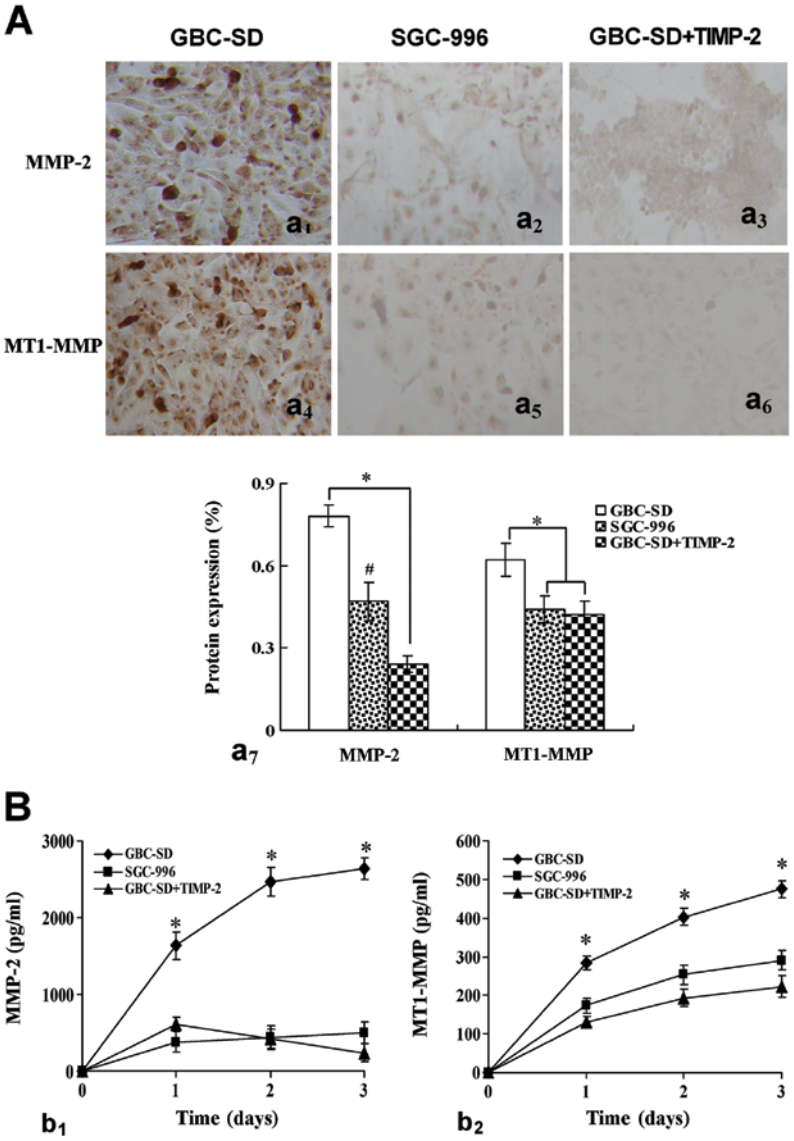

Figure 3. Expression of MMP-2, MT1-MMP proteins from sections [(A) SABC method, original magnification, x200] and supernates [(B) ELISA] of 3-D culture samples *in vitro* in GBC-SD, SGC-996 and GBC-SD+TIMP-2 groups. (A) The positive expression site of MMP-2 and MT1-MMP proteins presented yellow-brown reactant in the cytoplasm. Overexpression of MMP-2 (a_1) and MT1-MMP (a_4) proteins in GBC-SD group was observed. Expression of MMP-2 and MT1-MMP proteins in SGC-996 group ($a_{2,5}$) and GBC-SD+TIMP-2 ($a_{3,6}$) group was significantly decreased ($^*P<0.001$, $^\#P<0.01$, vs. GBC-SD group). (B) Expression of MMP-2 (b_1) and MT1-MMP (b_2) proteins in GBC-SD group increased significantly with time, when compared with SGC-996 group and GBC-SD+TIMP-2 group ($^*P<0.001$).

optimal structure formation achieved by 2 weeks. However, poorly aggressive SGC-996 cells were unable to form tubular-like structures with the same conditions (Fig. $1Ab_{1-4}$). SEM clearly visualized channelized or hollowed vasculogenic-like networks in GBC-SD cells (Fig. $1Ba_{1,2}$), with clear microvilli and tubular structures surrounding a cluster of tumor cells. TEM showed some microvilli outside the network, clear cellular organelle structures and cell connection with an increased electron density (Fig. $1Bb_1$). The results were concordant with our previous report (36). It is interesting that in the process of vasculogenic-like structure formation, using TIMP-2 (Fig. $1Ac_{1-4}$) for 2 days, GBC-SD cells lost the capacity of network formation, with visible cell aggregation, floating, nuclear fragmentation, apoptosis and necrosis. Using TIMP-2 for 48 h after network formation, the formed vasculogenic-like structures were destroyed, with visible cell aggregation, floating, nuclear fragmentation and apoptosis. It was shown that TIMP-2 inhibited and destroyed formation of VM, and formed-VM from the 3-D culture of GBC-SD cells *in vitro*.

Tumor growth and VM formation of GBC-SD xenografts in vivo. In the experiment, the tumor appeared gradually in the subcutaneous area of right axilback of nude mice from the 6th day after inoculation. As shown in Fig. 2A, xenograft formation rate in nude mice after 2 weeks was 100% (7/7) for GBC-SD, 71.4% (5/7) for SGC-996 and 33.3% (2/6) for GBC-SD+TIMP-2, with significant difference between GBC-SD group and GBC-SD+TIMP-2 group ($P<0.01$). In addition, the medium volume of nude mouse xenografts at 6th weeks in GBC-SD+TIMP-2 group was smaller than that of GBC-SD group (1.85+0.93 vs. 2.95+1.43 cm^3, $P<0.001$), but there was no significant difference between GBC-SD group and SGC-996 group ($P>0.05$).

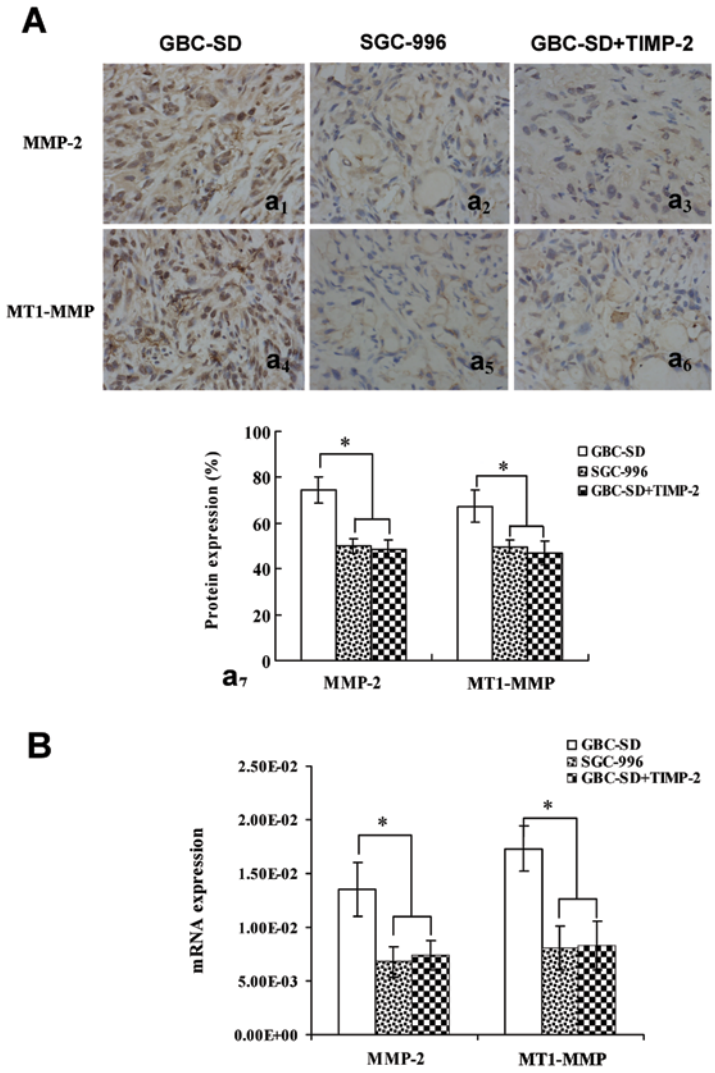

Figure 4. Expression of MMP-2, MT1-MMP proteins/mRNAs from sections of tumor xenografts *in vivo* [(A) SABC method, original magnification, x200; (B) qRT-PCR)] in GBC-SD, SGC-996 and GBC-SD+TIMP-2 groups. Overexpression of MMP-2 ($Aa_{1,7}$) and MT1-MMP ($Aa_{4,7}$) proteins or mRNA (B) in GBC-SD group was observed *in vivo*. Expression of MMP-2 and MT1-MMP proteins or mRNA in SGC-996 group ($Aa_{2,5,7}$ and B) and GBC-SD+TIMP-2 ($Ac_{3,6,7}$ and B) group was significantly decreased (*P<0.001, vs. GBC-SD group).

Morphology characteristics of xenografts were observed via H&E staining and dual-staining with CD31-PAS under optical microscopy and TEM. Microscopically, the xenografts in GBC-SD group showed that tumor cells lined channels containing red blood cells (Fig. $2Ba_1$) without any evidence of tumor necrosis; the channel consisted of tumor cells was negative for CD31 and positive for PAS; and tumor cells formed vessel-like structures with single red blood cell inside (Fig. $2Ba_2$). VM positive rate was 85.7% (6/7) in GBC-SD group. Among 24 tissue sections, 10 high-power fields in each section were counted to estimate the proportion of vessels that were lined by tumor cells, 5.7% (17/300) channels were seen to contain red blood cells among these tumor cell-lined vasculatures. In the central area of the tumor, xenografts exhibited VM in the absence of ECs, central necrosis or fibrosis (Fig. $2Ba_2$). For xenografts in GBC-SD group, TEM clearly showed single, double and several red blood cells existed in the centre of tumor nests (Fig. $2Ba_3$). There was no vascular structure between the surrounding tumor cells and erythrocytes. Neither necrosis nor fibrosis was observed in the tumor nests (Fig. $2Ba_3$). However, similar phenomenon failed to occur in xenografts of SGC-996 group (Fig. $2Bb_{1\text{-}3}$) or GBC-SD+TIMP-2 group (Fig. $2Bc_{1\text{-}3}$) with damaged cellular organelles, cell necrosis, nuclear pyknosis, fragmentation and apoptotic bodies (Fig. $2Bb_3$ and c_3). These findings demonstrated VM in GBC-SD nude mouse xenografts, was concordant with the results *in vivo* and in clinical report by us (34,36). Additionally, TIMP-2 was able to inhibit the VM formation of GBC-SD xenografts in nude mice *in vivo*.

Expression of MMP-2, MT1-MMP proteins/mRNAs in vitro and in vivo. Expression of MMP-2 and MT1-MMP proteins/mRNAs from sections and supernates of 3-D culture samples *in vitro* and from sections of tumor xenografts *in vivo* was shown in Figs. 3 and 4. The positive expression site of MMP-2 and MT1-MMP proteins presented yellow-brown reactant in the cytoplasm. Overexpression of MMP-2 (Fig. $3A_{a1,7}$) and MT1-MMP (Fig. $3Aa_{4,7}$) proteins in GBC-SD group was observed *in vitro*. Expression of MMP-2 and MT1-MMP proteins in SGC-996 group (Fig. $3Aa_{2,5,7}$) and GBC-SD+TIMP-2 (Fig. $3Aa_{3,6,7}$)

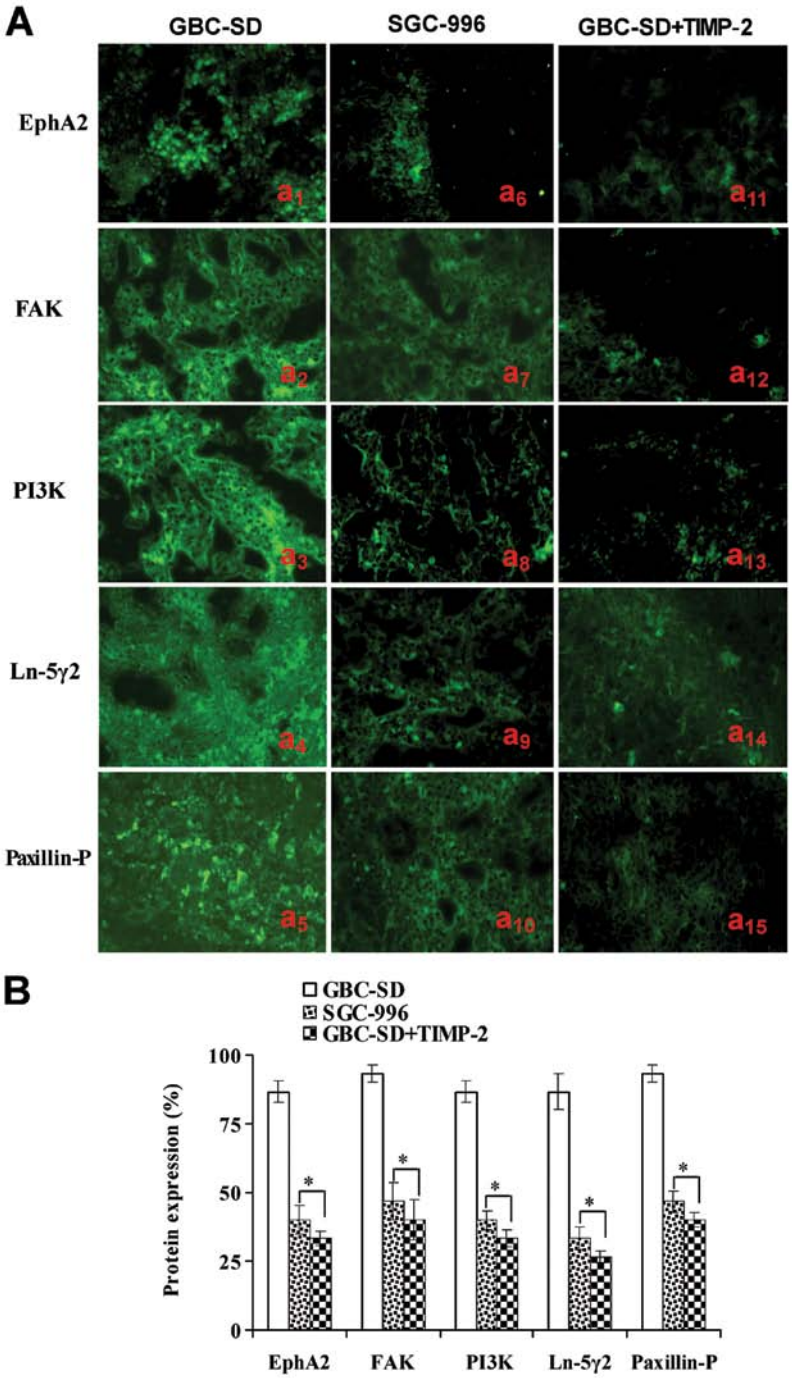

Figure 5. Expression of VM signal-related proteins EphA2, FAK, PI3K, Ln-5γ2 and Paxillin-P of the xenografts of each group *in vivo* (indirect immunofluorescence method, original magnification, x400). (A) Expression of EphA2, FAK, PI3K, Ln-5γ2 and Paxillin-P proteins of the xenografts in GBC-SD ($a_{1\text{-}5}$), SGC-996 ($a_{6\text{-}10}$) and GBC-SD+TIMP-2 ($a_{11\text{-}15}$) groups. The positive expression site of these proteins presented bright yellow-green fluorescent staining reactant in the cytoplasm. Expression of these proteins in GBC-SD group ($Aa_{1\text{-}5}$ and B) was markedly upregulated. However, expression of these proteins in SGC-996 ($Aa_{6\text{-}10}$ and B) and GBC-SD+TIMP-2 ($Aa_{10\text{-}15}$ and B) groups was significantly downregulated ($^{*}P<0.001$, vs. GBC-SD group).

group was significantly decreased ($^{*}P<0.001$, $^{\#}P<0.01$, vs. GBC-SD group). Moreover, expression of MMP-2 (Fig. $3Bb_1$) and MT1-MMP (Fig. $3Bb_2$) proteins from supernates of 3-D culture samples *in vitro* in GBC-SD group increased significantly with time, when compared with SGC-996 group and GBC-SD+TIMP-2 group ($^{*}P<0.001$). Furthermore, overexpression of MMP-2 (Fig. $4A_{a1,7}$ and B) and MT1-MMP (Fig. $4Aa_{4,7}$ and B) proteins or mRNAs from sections of tumor xenografts *in vivo* in GBC-SD group was also observed; expression of MMP-2 and MT1-MMP proteins or mRNAs in SGC-996 group (Fig. $4A_{a2,5,7}$ and B) and GBC-SD+TIMP-2 group (Fig. $4Aa_{3,6,7}$ and B) was significantly decreased ($^{*}P<0.001$, vs. GBC-SD group). The results showed that highly aggressive GBC-SD cells formed *in vitro* and *in vivo* VM networks overexpressing MMP-2 and MT1-MMP; however, poorly aggressive SGC-996 cells or GBC-SD cells treated by TIMP-2, which did not form these networks, markedly downregurated expression of MMP-2 and MT1-MMP. Thus, TIMP-2 effectively inhibit expression

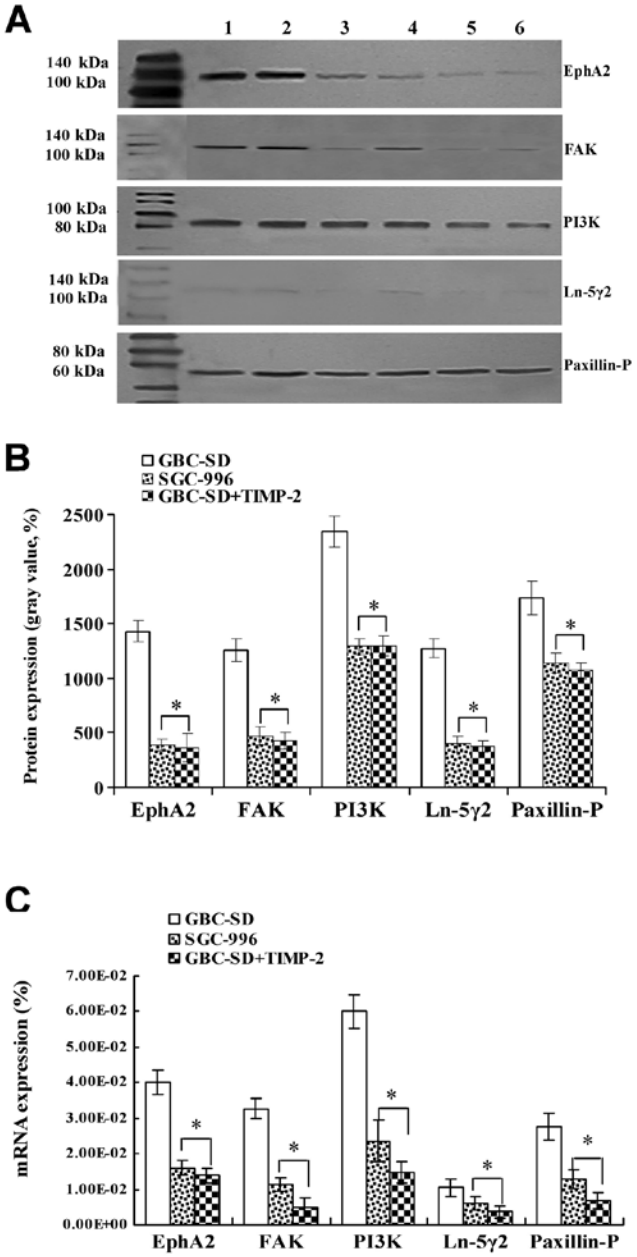

Figure 6. Expression of VM signal-related proteins/mRNAs EphA2, FAK, PI3K, Ln-5γ2 and Paxillin-P of the xenografts of each group *in vivo* [(A and B) western blotting; lanes 1 and 2, GBC-SD group; lanes 3 and 4, SGC-996 group; lanes 5 and 6, GBC-SD+TIMP-2 group. (C) qRT-PCR)]. (A and B) Overexpression of EphA2, FAK, PI3K, Ln-5γ2 and Paxillin-P proteins of the xenografts in GBC-SD group was observed; but expression of these proteins in SGC-996 or GBC-SD+TIMP-2 group was significantly decreased (*P<0.001). (C) Expression of EphA2, FAK, PI3K, Ln-5γ2 and Paxillin-P mRNAs of the xenografts in GBC-SD group was increased significantly when compared with SGC-996 and GBC-SD+TIMP-2 groups (*P<0.01).

of these proteins, inhibiting VM of GBC-SD cells *in vitro* and *in vivo*, as to disproof that highly aggressive GBC-SD cells formed *in vitro* and *in vivo* VM through the upreguration of MMP-2 and MT1-MMP expression.

Expression of EphA2, FAK, PI3K, Ln-5γ2 and Paxillin-P proteins/mRNAs of the tumor xenografts in vivo. Expression of EphA2, FAK, PI3K, Ln-5γ2 and Paxillin-P proteins/mRNAs of the xenografts of each group *in vivo* are shown in Figs. 5 and 6. Expression (bright yellow-green fluorescent staining reactant in the cytoplasm, or western gray value) of EphA2, FAK, PI3K, Ln-5γ2 and Paxillin-P proteins in GBC-SD group (Figs. $5A_{a1\text{-}5}$ and B and 6A and B) was all upregulated markedly; however, expression of these VM signal-related proteins in SGC-996 (Figs. $5Aa_{6\text{-}10}$ and B and 6A and B) and GBC-SD+TIMP-2 (Figs. $5Aa_{10\text{-}15}$ and B and 6A and B) groups was significantly downregulated (*P<0.001). Furthermore, expression of EphA2, FAK, PI3K, Ln-5γ2 and Paxillin-P mRNAs in GBC-SD group (Fig. 6C) was increased significantly when compared with SGC-996 group and GBC-SD+TIMP-2 group (*P<0.01). The results showed that highly aggressive GBC-SD cells formed *in vivo* VM networks overexpressing VM signal-related markers EphA2, FAK, PI3K, Ln-5γ2 and Paxillin-P; poorly aggressive SGC-996 cells, which did not form these networks, markedly downregurated expression of these VM signal-related markers; TIMP-2 effectively inhibit expression of these VM signal-related markers, then, as to disproof that highly aggressive GBC-SD cells formed *in vivo* VM through EphA2/FAK/Paxillin signaling and PI3K/MMPs/Ln-5γ2 signaling. Thus, we deduced that EphA2/FAK/Paxillin and PI3K/MMPs/Ln-5γ2 signaling pathways contributed to tumor growth and vasculogenic mimicry of human gallbladder carcinoma GBC-SD cells *in vitro* and *in vivo*.

Discussion

VM is a novel paravascular tumor blood supply pattern in some highly aggressive malignant tumors formed by tumor cells instead of endothelial cells. VM describes the unique ability of highly aggressive tumor cells to express endothelial cell-associated genes and form ECM-rich, patterned tubular networks when cultured on a three-dimensional matrix. We previously reported that VM existed in human gallbladder carcinomas and correlated with the patient's poor prognosis (34,35). In this study, we further investigated vasculogenic-like network formation capability of human gallbladder carcinomas *in vitro* and *in vivo*. The results shown that highly aggressive GBC-SD cells were able to form vasculogenic-like network structures when cultured on Matrigel and rat-tail collagen type I and when injected subcutaneously into the right axilback of nu/nu mice and then facilitated growth of tumor cells or xenografts; that poorly aggressive SGC-996 cells were unable to form the tubular-like structures with the same conditions; and TIMP-2 was able to inhibit and destroy formation of VM from the 3-D culture of GBC-SD cells *in vitro* and VM formation of GBC-SD xenografts in nude mice *in vivo*, thus inhibiting tumor xenografts' growth. The results were not only concordant with our previous report (36), but also further confirmed vasculogenic-like network formation capability of highly aggressive GBC-SD cells *in vitro* and *in vivo*.

The molecular events underlying VM displayed by highly aggressive malignant tumor cells, especially, aggressive human gallbladder carcinomas remain poorly understood. Therefore, understanding the key molecular mechanisms that regulate VM in human gallbladder carcinomas would be an important event and provide potential targets for new therapies of gallbladder carcinomas. Recently, experimental evidence has shown the importance of several key molecules or signaling

pathways in the formation of vasculogenic-like networks by aggressive malignant tumor cells, including EphA2, FAK (25-29), PI3K, MMPs, and Ln-5γ2 chain (21-24).

PI3K/MMPs/Ln-5γ2 signaling pathway is a key pathway which regulate VM formation of aggressive malignant tumor cells. PI3K, made up of four different 110-kDa catalytic subunits and a smaller regulatory subunit, is a lipid kinase that phosphorylates phosphatidylinositol or its derivatives on the 3-hydroxyl of the inositol head group. The principle product of PI3K activity, PI (3-5) -P3 acts as a binding site for many intracellular proteins that include pleckstrin homology (PH) domains with selectivity for this lipid. The PI3K signaling pathway plays an integral role in many normal cellular processes, including survival, proliferation, differentiation, metabolism and motility, in a variety of cell types (37). MMPs, divided into soluble MMPs and MT-MMP, is a broad family of zinc-biding endopeptidases that participate in the ECM degradation that accompanies cancer cell invasion, metastasis and angiogenesis (38-41). Specifically, MT1-MMP and MMP-2 are key mediators of invasion, metastasis, tumor angiogenesis and recently tumor cell VM (22,42). Numerous studies have indicated that MT1-MMP is important for endothelial tubulogenesis in fibrin gels (43), in endothelial cell migration on 3-D collagen gels (44) and both MT1-MMP and MMP-2 are upregulated when endothelial cells are cultured on a 3-D matrix (45). Recent multiple studies have indicated that MMP-2 and MT1-MMP expression was significantly related to VM formation in melanoma and ovarian carcinoma cells in 3-D culture (21,24). Microarray analysis revealed that MMPs (-1, -2, -9 and -14) were all more highly expressed in aggressive melanoma with VM channels compared with poorly aggressive melanoma with absence of VM (46). The Ln-5γ2 chain, MMP-2 and MT1-MMP act cooperatively and required highly aggressive melanoma tumor cells to engage in VM when cultured on a three-dimensional ECM (22). The Ln-5γ2 chain in the ECM is able to remote VM formation (22,23). Recent observation showed that highly aggressive melanoma tumor cells can secrete the Ln-5γ2 chain and that the γ2 and γ2x chains, antisense oligonucleotides to the Ln-5γ2 chain and antibodies to MMP-2 or MT1-MMP may inhibit VM formation. Several recently published reports have indicated that PI3K is an important adjustor of directly affecting the cooperative interactions of MT1-MMP and MMP-2 activity in highly aggressive melanoma tumor cells. PI3K regulates MT1-MMP activity, which promotes the conversion of pro-MMP into its active conformation through an interaction with TIMP-2. Both enzymatically active MT1-MMP and MMP-2 may therefore promote the cleavage of Ln-5γ2 chain into pro-migratory γ2 and γ2x fragments. The deposition of these fragments into tumor extracellular milieu may result in increased migration, invasion and VM formation (22,23). Special inhibitors of PI3K may impair VM formation and decrease MT1-MMP and MMP-2 activity. Furthermore, inhibition of PI3K blocked the cleavage of Ln-5γ2 chain, resulting in decreased levels of the γ2 and γ2x promigratory fragments (21). Similarly, in aggressive ovarian tumor cells, MMP-2 or MT1-MMP seems to play an important role in the VM channel. Human ovarian cancers with MMP overexpression are more likely to have tumor cell-lined vasculature (24). Thus, PI3K/MMPs/Ln-5γ2 may represent the predominant targets for anti-VM of tumors and cancer therapy. In this study, expression of MMP-2 and MT1-MMP proteins/mRNAs from sections and supernates of 3-D culture samples *in vitro* and from sections of tumor xenografts *in vivo* in GBC-SD group was upregulated significantly ($P<0.001$); however, expression of MMP-2 and MT1-MMP proteins/mRNAs in SGC-996 group was significantly downregulated ($P<0.001$). Furthermore, expression of PI3K and Ln-5γ2 proteins/mRNAs of the xenografts of GBC-SD group *in vivo* was also upregulated markedly; however, expression of these VM signal-related proteins in SGC-996 groups was significantly downregulated ($P<0.001$). These results showed that highly aggressive GBC-SD cells formed *in vitro* and *in vivo* VM networks overexpressing VM signal-related markers PI3K, MMP-2, MT1-MMP and Ln-5γ2; poorly aggressive SGC-996 cells, which did not form these networks, markedly downregurated expression of these VM signal-related markers. Thus, we deduced that highly aggressive GBC-SD cells formed VM *in vitro* and *in vivo* through the upregulation of PI3K/MMPs/Ln-5γ2 signaling, that PI3K/MMPs/Ln-5γ2 signaling pathway contributed to tumor growth and VM of human gallbladder carcinomas.

EphA2/FAK/Paxillin signaling pathway is another key pathway which regulated VM formation of aggressive malignant tumor cells. EphA2, a receptor tyrosine kinase and a member of the Eph (ephrin receptor) family of protein tyrosine kinases (PTKs) which could be pivotal factors of VM, has been found to play an important role in angiogenesis and in the process of formation of VM (24,28,47,48). Microarray analyses revealed that EphA2 were dramatically overexpressed in aggressive human cutaneous and uveal melanoma cells, although not in poorly aggressive melanoma cells. Transient knockout of EphA2 *in vitro* abrogated the ability of highly aggressive melanoma cells to form the vasculogenic-like networks (25,49). EphA2 upstream molecules regulate VM formation. EphA2 and VEcad are colocalized at sites of cell-cell adhesion. Knockdown of EphA2 expression does result in a redistribution of EphA2 on the cell membrane and an inability of the cells to form vasculogenic structures. When organized on the cell membrane, EphA2 is capable of binding to its ligand EphA1, resulting in the phosphorylation of EphA2. Phosphorylated EphA2 then forms an interaction with FAK, which leads to phosphorylation and activation of FAK (49). Additionally, EphA2 may converge to activate the PI3K (as effector of EphA2 downstream) pathway leading to the activation of MMP-2 and consequent cleavage of Ln-5γ2 (25-27,50,51). Also, the localization of EphA2 in aggressive human melanoma tissues is associated with areas containing patterns of vasculogenic-like networks. FAK, non-receptor protein tyrosine kinase, is a 125-kDa cytoplasmic tyrosine kinase associated with focal adhesions and is the major protein to become tyrosine phosphorylated after integrin activation. Recently, studies have demonstrated FAK to be an important key mediator of the aggressive melanoma phenotype, including VM (28,29). FAK is phosphorylated on Tyr^{397} and Tyr^{576} in aggressive human cutaneous and uveal melanoma cells cultured on a 3-D matrix *in vitro*, as well as in radial and vertical growth phase melanomas *in situ*. Expression of FAK-related non-kinase in melanoma cells, which acts to disrupt FAK signaling, directly results in the inhibition of the

aggressive phenotype, as demonstrated by decreased invasion, migration and VM potential. FAK signaling regulates invasion, migration and VM through two distinct signaling pathways. Firstly, FAK signals through Erk1/2 increase the levels of urokinase activity, thus regulating invasion of the aggressive melanoma cells. Additionally, FAK seems to signal through unknown downstream effectors to promote migration in aggressive melanoma cells that may contribute to an increase of VM potential. Secondly, Erk1/2 regulates MMP-2 and MT1-MMP activity, thus promoting melanoma invasion and VM (28,29). Collectively, these observations implicate FAK as a promoter of the aggressive melanoma phenotype, thereby identifying it as a rational target for therapeutic intervention of malignant melanoma. Paxillin is a focal adhesion-associated, phosphotyrosine-containing protein that may play a role in numerous signaling pathways. Paxillin contains a number of motifs as docking sites that mediate protein-protein interactions. Thus paxillin itself serves as a docking protein to recruit signaling molecules to a specific cellular compartment, the focal adhesions and/or to recruit specific combinations of signaling molecules into a complex to coordinate downstream signaling. The biological function of paxillin coordinated signaling is likely to regulate cell spreading and motility. Also, FAK plays an important role in tyrosine phosphorylation of Paxillin (52). In VM, activity of FAK, as bridging protein between EphA2 and integrins, mediates Paxillin phosphorylation at local adhesion sites, then regulating focal adhesion effect, increasing tumor cell mobility, being conducive to the formation of VM (48). So, EphA2/FAK/Paxillin signaling pathway may represent other predominant targets for anti-VM of tumors and cancer therapy. In this study, expression (bright yellow-green fluorescent staining reactant in cytoplast, or western gray value) of EphA2, FAK and Paxillin-P proteins/mRNAs of the xenografts in GBC-SD group was upregulated markedly; however, expression of these VM signal-related proteins in SGC-996 and GBC-SD+TIMP-2 groups was significantly downregulated (all $P<0.001$). The results showed that highly aggressive GBC-SD cells formed *in vivo* VM networks overexpressing VM signal-related markers EphA2, FAK and Paxillin-P; poorly aggressive SGC-996 cells, which did not form these networks, significantly downregurated expression of these VM signal-related markers. Thus, we deduced that highly aggressive GBC-SD cells formed VM *in vitro* and *in vivo* through the upregulation of EphA2/FAK/Paxillin signaling, and that EphA2/FAK/Paxillin signaling pathways also contributed to tumor growth and VM of human gallbladder carcinomas.

TIMP-2 is a 21-kDa protein which selectively forms a complex with the latent proenzyme form of the 72-kDa type IV collagenase. The secreted protein has 194 amino acid residues and is not glycosylated. TIMP-2 inhibits at a 1:1 ratio the type IV collagenolytic activity and the gelatinolytic activity associated with the 72-kDa enzyme. Whereas the 72-kDa type IV collagenase is a member of the collagenase enzyme family that has been closely linked with the invasive phenotype of cancer cells. Both normal cells and highly invasive tumor cells produce the 72-kDa type IV procollagenase enzyme in a complexed form consisting of the proenzyme and TIMP-2. The balance between activated enzyme and available inhibitor is considered to be a critical determinant of the matrix proteolysis associated with a variety of pathologic processes, including tumor cell invasion. TIMP-2 is capable of binding to both the latent and activated forms of the 72-kDa type IV collagenase and will abolish the hydrolytic activity of all members of the metalloproteinase family (53,54). TIMP-2 is a potent inhibitor of cancer cell invasion through reconstituted extracellular matrix (55,56). TIMP-2 produced by the same tumor cells which make collagenase, therefore, exists as a natural suppressor of invasion. Addition of endogenous inhibitor TIMP-2 or antibodies to 72-kDa type IV collagenase or specific antiserum against the 72-kDa type IV collagenase achieved alteration of the type IV collagenase-inhibitor balance, then inhibited HT-1080 cell invasion (55). A significantly higher concentration of TIMP-2 may effectively inhibit all of the proteolytic activities associated with MMP-2 and/or MT1-MMP (plus other MMPs in the culture that can bind TIMP-2). The inhibition of either MMP-2 or MT1-MMP activity with antibodies is sufficient to prevent formation of vasculogenic-like patterned networks (22). To determine whether MMPs, especially MMP-2 or MT1-MMP are actively involved and required for the vasculogenic process of 3-D culture matrices *in vitro* and tumor xenografts *in vivo*, recombinant TIMP-2 was added to the highly aggressive GBC-SD cells in 3-D culture matrices and injected intratumorally into GBC-SD xenografts *in vivo*. The results indicated that all of untreated GBC-SD cells and xenografts formed patterned tubular networks within 2 weeks of seeding and injecting and expression of MMP-2, MT1-MMP and EphA2, FAK, PI3K, Ln-5γ2 proteins/mRNAs in these untreated GBC-SD cells and xenografts was upregulaed to different degree; whereas TIMP-2 retarded the onset of the patterned network formation and markedly downregurated expression of these proteins/mRNAs. Thus, we believed that TIMP-2 inhibited VM formation of GBC-SD cells *in vitro* and *in vivo* through two separate mechanisms. On one hand, TIMP-2 inhibited PI3K/MMPs/Ln-5γ2 signaling pathway through downregulation of MMP-2 and MT1-MMP expression. Inhibition of PI3K not only reduced MT1-MMP and MMP-2 activity, but also blocked the cleavage of Ln-5γ2 chain, resulting in decreased levels of the γ2 and γ2x promigratory fragments and impairment of VM formation. On the other hand, TIMP-2 indirectly inhibited EphA2/FAK/Paxillin signaling pathway through downregulation of EphA2 and FAK expression. Inhibition of EphA2 and FAK through Erk1/2 not merely decreased the levels of urokinase activity, thus regulating loss of the invasive ability of aggressive GBC-SD cells, but also downregulated MMP-2 and MT1-MMP activity, inhibiting tumor invasion and VM (28,29). Additionally, inhibition of EphA2 did not converge to activate the PI3K pathway leading to the activation of MMP-2 and consequently blocked cleavage of Ln-5γ2 (25-27,50,51). Collectively, these results showed that TIMP-2 inhibited tumor growth and VM formation of GBC-SD cells *in vitro* and *in vivo* through diverse mechanisms; and served as to disproof that highly aggressive GBC-SD cells formed *in vitro* and *in vivo* VM through the upreguration of PI3K/MMPs/Ln-5γ2 signaling, especially MMP-2 and MT1-MMP expression.

In conclusion, highly aggressive GBC-SD cells formed VM *in vitro* and *in vivo* through the upregulation of PI3K/MMPs/Ln-5γ2 signaling and EphA2/FAK/Paxillin signaling.

PI3K/MMPs/Ln-5γ2 and EphA2/FAK/Paxillin signaling pathways contributed to tumor growth and VM of human gallbladder carcinomas. PI3K/MMPs/Ln-5γ2 and EphA2/FAK/Paxillin may act in a coordinated manner as key signaling pathways in the process of human gallbladder carcinoma VM and illustrate novel targets that could be potentially exploited for therapeutic intervention.

Acknowledgements

This study was supported by a grant from the National Nature Science Foundation of China (no. 30672073).

References

1. Gourgiotis S, Kocher HM, Solaini L, Yarollahi A, Tsiambas E and Salemis NS: Gallbladder cancer. Am J Surg 196: 252-264, 2008.
2. Lazcano-Ponce EC, Miquel JF, Muñoz N, Herrero R, Ferrecio C, Wistuba II, Alonso de Ruiz P, Aristi Urista G and Nervi F: Epidemiology and molecular pathology of gallbladder cancer. CA Cancer J Clin 51: 349-364, 2001.
3. Reddy SK and Clary BM: Surgical management of gallbladder cancer. Surg Oncol Clin North Am 18: 307-324, 2009.
4. Li LD, Zhang SW, Lu FZ, Mu R, Sun XD and Huangpu XM: Research on characteristics of mortality spectrum and type composition of malignant tumors in China. Zhonghua Zhongliu Zazhi 19: 323-328, 1997.
5. Hsing AW, Gao YT, Devesa SS, Jin F and Fraumeni JF Jr: Rising incidence of biliary tract cancers in Shanghai, China. Int J Cancer 75: 368-370, 1998.
6. Chakravarty KD, Yeh CN, Jan YY and Chen MF: Factors influencing long-term survival in patients with T3 gallbladder adenocarcinoma. Digestion 79: 151-157, 2009.
7. Konstantinidis IT, Deshpande V, Genevay M, Berger D, Fernandez-del Castillo C, Tanabe KK, Zheng H, Lauwers GY and Ferrone CR: Trends in presentation and survival for gallbladder cancer during a period of more than 4 decades: a single-institution experience. Arch Surg 144: 441-447, 2009.
8. Ishii H, Furuse J, Yonemoto N, Nagase M, Yoshino M and Sato T: Chemotherapy in the treatment of advanced gallbladder cancer. Oncology 66: 138-142, 2004.
9. Morise Z, Sugioka A, Tanahashi Y, Okabe Y, Ikeda M, Kagawa T and Takeura C: Treatment of patients with unresectable advanced carcinoma of biliary tract chemotherapy and surgical resection. Anticancer Res 29: 1783-1786, 2009.
10. Mahantshetty UM, Palled SR, Engineer R, Homkar G, Shrivastava SK and Shukla PJ: Adjuvant radiation therapy in gallbladder cancers: 10 years experience at Tata Memorial Hospital. J Cancer Res Ther 2: 52-56, 2006.
11. Mojica P, Smith D and Ellenhorn J: Adjuvant radiation therapy is associated with improved survival for gallbladder carcinoma with regional metastatic disease. J Surg Oncol 96: 8-13, 2007.
12. Shukla PJ and Barreto SG: Gallbladder cancer: we need to do better! Ann Surg Oncol 16: 2084-2085, 2009.
13. Maniotis AJ, Folberg R, Hess A, Seftor EA, Gardner LM, Pe'er J, Trent JM, Meltzer PS and Hendrix MJ: Vascular channel formation by human melanoma cells in vivo and in vitro: vasculogenic mimicry. Am J Pathol 155: 739-752, 1999.
14. Warso MA, Maniotis AJ, Chen X, Majumdar D, Patel MK, Shilkaitis A, Gupta TK and Folberg R: Prognostic significance of periodic acid-Schiff-positive patterns in primary cutaneous melanoma. Clin Cancer Res 7: 473-477, 2001.
15. Shirakawa K, Wakasugi H, Heike Y, Watanabe I, Yamada S, Saito K and Konishi F: Vasculogenic mimicry and pseudocomedo formation in breast cancer. Int J Cancer 99: 821-828, 2002.
16. Sood AK, Fletcher MS, Zahn CM, Gruman LM, Coffin JE, Seftor EA and Hendrix MJ: The clinical significance of tumor cell-lined vasculature in ovarian carcinoma: implications for anti-vasculogenic therapy. Cancer Biol Ther 1: 661-664, 2002.
17. Sun B, Zhang S, Zhang D, Du J, Guo H, Zhao X, Zhang W and Hao X: Vasculogenic mimicry is associated with high tumor grade, invasion and metastasis, and short survival in patients with hepatocellular carcinoma. Oncol Rep 16: 693-698, 2006.
18. Guzman G, Cotler SJ, Lin AY, Maniotis AJ and Folberg R: A pilot study of vasculogenic mimicry immunohistochemical expression in hepatocellular carcinoma. Arch Pathol Lab Med 131: 1776-1781, 2007.
19. Li M, Gu Y, Zhang Z, Zhang S, Zhang D, Saleem AF, Zhao X and Sun B: Vasculogenic mimicry: a new prognostic sign of gastric adenocarcinoma. Pathol Oncol Res 16: 259-266, 2010.
20. Baeten CI, Hillen F, Pauwels P, de Bruine AP and Baeten CG: Prognostic role of vasculogenic mimicry in colorectal cancer. Dis Colon Rectum 52: 2028-2035, 2009.
21. Hess AR, Seftor EA, Seftor RE and Hendrix MJ: Phosphoinositide 3-kinase regulates membrane Type 1-matrix metalloproteinase (MMP) and MMP-2 activity during melanoma cell vasculogenic mimicry. Cancer Res 63: 4757-4762, 2003.
22. Seftor RE, Seftor EA, Koshikawa N, Meltzer PS, Gardner LM, Bilban M, Stetler-Stevenson WG, Quaranta V and Hendrix MJ: Cooperative interactions of laminin 5 gamma 2 chain, matrix metalloproteinase-2, and membrane type-1-matrix/metalloproteinase are required for mimicry of embryonic vasculogenesis by aggressive melanoma. Cancer Res 61: 6322-6327, 2001.
23. Seftor RE, Seftor EA, Kirschmann DA and Hendrix MJ: Targeting the tumor microenvironment with chemically modified tetracyclines: inhibition of laminin 5 gamma2 chain promigratory fragments and vasculogenic mimicry. Mol Cancer Ther 1: 1173-1179, 2002.
24. Sood AK, Fletcher MS, Coffin JE, Yang M, Seftor EA, Gruman LM, Gershenson DM and Hendrix MJ: Functional role of matrix metalloproteinases in ovarian tumor cell plasticity. Am J Obstet Gynecol 190: 899-909, 2004.
25. Hess AR, Seftor EA, Gardner LM, Carles-Kinch K, Schneider GB, Seftor RE, Kinch MS and Hendrix MJ: Molecular regulation of tumor cell vasculogenic mimicry by tyrosine phosphorylation: role of epithelial cell kinase (Eck/EphA2). Cancer Res 61: 3250-3255, 2001.
26. Margaryan NV, Strizzi L, Abbott DE, Seftor EA, Rao MS, Hendrix MJ and Hess AR: EphA2 as a promoter of melanoma tumorigenicity. Cancer Biol Ther 8: 279-288, 2009.
27. Hess AR, Margaryan NV, Seftor EA and Hendrix MJ: Deciphering the signaling events that promote melanoma tumor cell vasculogenic mimicry and their link to embryonic vasculogenesis: role of the Eph receptors. Dev Dyn 236: 3283-3296, 2007.
28. Hess AR and Hendrix MJ: Focal adhesion kinase signaling and the aggressive melanoma phenotype. Cell Cycle 5: 478-480, 2006.
29. Hess AR , Postovit LM, Margaryan NV, Seftor EA, Schneider GB, Seftor RE, Nickoloff BJ and Hendrix MJ: Focal adhesion kinase promotes the aggressive melanoma phenotype. Cancer Res 65: 9851-9860, 2005.
30. Ruf W, Seftor EA, Petrovan RJ, Weiss RM, Gruman LM, Margaryan NV, Seftor RE, Miyagi Y and Hendrix MJ: Differential role of tissue factor pathway inhibitors 1 and 2 in melanoma vasculogenic mimicry. Cancer Res 63: 5381-5389, 2003.
31. Wang JY, Sun T, Zhao XL, Zhang SW, Zhang DF, Gu Q, Wang XH, Zhao N, Qie S and Sun BC: Functional significance of VEGF-a in human ovarian carcinoma: role in vasculogenic mimicry. Cancer Biol Ther 7: 758-766, 2008.
32. Ge CY and Fan YZ: Vasculogenic mimicry and its molecules signaling pathways. Chin Med Abstr (Surg) 15: 344-350, 2006.
33. Fan YZ and Sun W: Molecular regulation of vasculogenic mimicry in tumors and potential tumor-target therapy. World J Gastrointest Surg 2: 117-127, 2010.
34. Fan YZ, Sun W, Zhang WZ and Ge CY: Vasculogenic mimicry in human primary gallbladder carcinoma and clinical significance thereof. Zhonghua Yi Xue Za Zhi 87: 145-149, 2007.
35. Sun W, Shen ZY, Zhang H, Fan YZ, Zhang WZ, Zhang JT, Lu XS and Ye C: Overexpression of HIF-1α in primary gallbladder carcinoma and its relation to vasculogenic mimicry and unfavourable prognosis. Oncol Rep 27: 1990-2002, 2012.
36. Sun W, Fan YZ, Zhang WZ and Ge CY: A pilot histomorphology and hemodynamic of vasculogenic mimicry in gallbladder carcinomas in vivo and in vitro. J Exp Clin Cancer Res 30: 46, 2011.
37. Link W, Rosado A, Fominaya J, Thomas JE and Carnero A: Membrane localization of all class I PI3-kinase isoforms suppresses c-Myc-induced apoptosis in Rat1 fibroblasts via Akt. J Cell Biochem 95: 979-989, 2005.
38. McCawley LJ and Matrisian LM: Matrix metalloproteinases: multifunctional contributors to tumor progression. Mol Med Today 6: 149-156, 2000.

39. Noel A, Gilles C, Bajou K, Devy L, Kebers F, Lewalle JM, Maquoi E, Munaut C, Remacle A and Foidart JM: Emerging roles for proteinases in cancer. Invasion Metastasis 17: 221-239, 1997.
40. Stetler-Stevenson WG: Matrix metalloproteinases in angiogenesis: a moving target for therapeutic intervention. J Clin Invest 103: 1237-1241, 1999.
41. Seiki M: Membrane-type matrix metalloproteinases. APMIS 107: 137-143, 1999.
42. Chang C and Werb Z: The many faces of metalloproteases: cell growth, invasion, angiogenesis and metastasis. Trends Cell Biol 11: S37-S43, 2001.
43. Lafleur, MA, Handsley MM, Knauper V, Murphy G and Edwards DR: Endothelial tubulogenesis within fibrin gels specifically requires the activity of membrane-type-matrix metalloproteinases (MT-MMPs). J Cell Sci 115: 3427-3438, 2002.
44. Koike T, Vernon RB, Hamner MA, Sadoun E and Reed MJ: MT1-MMP, but not secreted MMPs, influences the migration of human microvascular endothelial cells in 3-dimensional collagen gels. J Cell Biochem 86: 748-758, 2002.
45. Haas TL, Davis SJ and Madri JA: Three-dimensional type I collagen lattices induce coordinate expression of matrix metalloproteinases MT1-MMP and MMP-2 inmicrovascular endothelial cells. J Biol Chem 273: 3604-3610, 1998.
46. Hendrix MJ, Seftor EA, Kirschmann DA, Quaranta V and Seftor RE: Remodeling of the microenvironment by aggressive melanoma tumor cells. Ann NY Acad Sci 995: 151-161, 2003.
47. Brantley DM, Cheng N, Thompson EJ, Lin Q, Brekken RA, Thorpe PE, Muraoka RS, Cerretti DP, Pozzi A, Jackson D, Lin C and Chen J: Soluble Eph A receptors inhibit tumor angiogenesis and progression in vivo. Oncogene 21: 7011-7026, 2002.
48. Cheng N, Brantley DM, Liu H, Lin Q, Enriquez M, Gale N, Yancopoulos G, Cerretti DP, Daniel TO and Chen J: Blockade of EphA receptor tyrosine kinase activation inhibits vascular endothelial cell growth factor-induced angiogenesis. Mol Cancer Res 1: 2-11, 2002.
49. Miao H, Burnett E, Kinch M, Simon E and Wang B: Activation of EphA2 kinase suppresses integrin function and causes focal-adhesion-kinase dephosphorylation. Nat Cell Biol 2: 62-69, 2000.
50. Hendrix MJ, Seftor EA, Meltzer PS, Gardner LM, Hess AR, Kirschmann DA, Schatteman GC and Seftor RE: Expression and functional significance of VE-cadherin in aggressive human melanoma cells: role in vasculogenic mimicry. Proc Natl Acad Sci USA 98: 8018-8023, 2001.
51. Hess AR, Seftor EA, Gruman LM, Kinch MS, Seftor RE and Hendrix MJ: VE-cadherin regulates EphA2 in aggressive melanoma cells through a novel signaling pathway: implications for vasculogenic mimicry. Cancer Biol Ther 5: 228-233, 2006.
52. Schaller MD: Paxillin: a focal adhesion-associated adaptor protein. Oncogene 20: 6459-6472, 2001.
53. Stetler-Stevenson WG, Krutzsch HC and Liotta LA: TIMP-2, a new member of the metalloproteinase inhibitor family. J Biol Chem 264: 17374-17378, 1989.
54. Goldberg GI, Marmer BL, Grant GA, Eisen AZ, Wilhelm S and He C: Human 72-kDa type IV collagenase forms a complex with a tissue inhibitor of metalloproteinase inhibitor. Proc Nati Acad Sci USA 86: 8207-8211, 1989.
55. Albini A, Melchiori A, Santi L, Liotta LA, Brown PD and Stetler-Stevenson WG: Tumor cell invasion inhibited by TIMP-2. J Natl Cancer Inst 83: 775-779, 1991.
56. Liotta LA and Stetler-Stevenson WG: Tumor invasion and metastasis: an imbalance of positive and negative regulation. Cancer Res 51 (Suppl): S5054-S5059, 1991.